Design of a Series Elastic Humanoid for the DARPA Robotics Challenge

Coleman Knabe, John Seminatore, Jacob Webb, Michael Hopkins,
Tomonari Furukawa, Alexander Leonessa*, and Brian Lattimer

***Abstract*— This paper describes the mechanical design of ESCHER, a series elastic humanoid developed to compete in the DARPA Robotics Challenge (DRC). The design methodology was informed by preliminary experimental results obtained using the THOR humanoid, a prototype platform developed for the DRC Trials, relying heavily on an accurate model of the torque-controlled robot in the Gazebo simulation environment. The redesigned lower body features a unique double actuated knee; by driving the single degree of freedom joint with two identical linear series elastic actuators (SEAs), the lower body is able to meet the necessary speed and torque requirements for locomotion on rough terrain. Experimental results demonstrating ESCHER's ability to step onto a 23 cm block, representative of the stairs task at the DRC Finals, validating the proposed approach. Joint torques measured on the hardware platform approximate those in simulation, validating the proposed design methodology.**

I. Introduction

Design of bipedal robots is a difficult, iterative process requiring consideration of overall functionality as well as operation environment. The Tactical Hazardous Operations Robot (THOR), in Fig. 1a, was developed for the DARPA Robotics Challenge (DRC) trials with emphasis placed on using mechanisms to achieve human-like range of motion and to walk on unstructured terrain. For the DRC finals, however, THOR lacked the necessary torque to complete all the tasks, including stairs and rough terrain. This prompted the design of the Electric Series Compliant Humanoid for Emergency Response (ESCHER), in Fig. 1b, to address these limitations. As desired functionality increases, it is quite possible to enter into a design loop where additional mass can overwhelm power and actuation systems or reduce payload capacity to unacceptable levels. As a result, proper actuator selection is critical to meeting performance goals.

While many approaches exist to aid in the development of complex systems, robot design strategies are not well documented in literature. One approach used by exoskeletons such as BLEEX [1] and CADEN–7 [2] uses measured joint torque and angle data from human kinematics studies to determine motor specifications. Humanoid designs intrinsically mimic the human form, though the design process tends to vary from platform to platform. Bipeds such as WABIAN [3] and LOLA [4] were designed using an open-ended cyclic methodology, deriving link inertias from a detailed CAD model after each design milestone and testing in simulation to iteratively refine joint specifications. The HRP–4 [5] and TORO [6] platforms are the result of gradual evolution over years of development, improving identified limitations of previous designs. The design process of NAO [7] avoided iteration and instead selected actuators based on a simulation model with reduced degrees of freedom and simplified kinematics, tested through dynamic motions in both the sagittal and frontal planes. Validated tools to support robot design have the potential to accelerate the development of new robots.

The authors are with the Terrestrial Robotics, Engineering & Controls (TREC) Laboratory at Virginia Tech.

*This material is based upon work supported by (while serving at) the National Science Foundation.

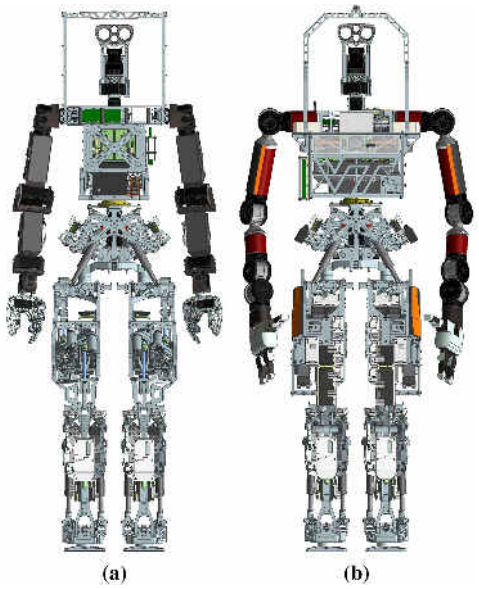

Fig. 1. (a) Tactical Hazardous Operations Robot (THOR) and (b) Electric Series Compliant Humanoid for Emergency Response (ESCHER).

This paper overviews the design process and validation of the ESCHER platform. Section II provides an approach for creating an accurate model of a torque-controlled robot in the Gazebo simulator and for using simulation to generate reliable design requirements. Section III contains an overview of the ESCHER platform and details the design of the thigh subsystem. Section IV contains data on the new double series elastic actuator (SEA) control design, as well as experimental results from software and hardware testing which validate the thigh upgrade.

II. Simulated Robot Model

A well-designed simulator enables rapid development and testing of algorithms; it can also be a tool used for the design of future robots. This section describes the framework used to develop a dynamic model of a series elastic humanoid

and its use as a tool to determine design specifications for ESCHER.

A. Model Development

Gazebo is a powerful 3D physics simulator utilizing the Open Dynamics Engine (ODE) to solve complex dynamic equations of motion, offering the ability to accurately and efficiently simulate robots in both indoor and outdoor environments [8]. There is an intrinsic trade-off between the accuracy, fidelity, and performance of a simulated system, so it is important to be cautious of each approximation that is made during model construction to avoid compromising model integrity.

On hardware, joint torques are regulated using inline actuator load cell force measurements which are converted using Jacobian matrices under a quasi-static joint assumption. Thus, THOR and ESCHER are similarly modelled using a rigid body model with ideal torque sources at each joint, an approach commonly taken for modelling torque-controlled robots [9–13]. Aside from bandwidth limitations, the SEAs used on each robot are strong approximators of a pure torque source [14], so the Gazebo model provides sufficient performance without requiring a model of each actuator subsystem.

Dynamic accuracy of the model is strongly dependent on the accuracy of link inertia definitions. For both THOR and ESCHER models, individual link inertias are generated from a detailed CAD model built in Siemens NX. Each component on the robot is modelled using a custom density calculated from the part's measured mass and CAD volume. However, CAD model does not include wires or wire weight, so defined body link masses of the simulation model are increased proportionally in the head, chest, and legs to match the overall hardware mass. For the initial design of ESCHER, a mass margin of 10% was allowed and distributed over the body. This method is easy to implement, yet is sensitive enough to model mass distributions and moments of inertia without requiring experimental identification of inertial parameters or link dynamics.

One identified pitfall associated with Gazebo is a convergence issue in ODE when there are large mass ratios between body links. The frame architectures for THOR and ESCHER use universal joints at the 2-DOF hip roll/yaw and ankle pitch/roll joints, where a small lightweight trunnion connects two large body links. These extreme mass ratios caused numerical instability in the Gazebo ODE solver. To amend this problem, mass and inertia were gradually increased on each trunnion until the simulator converged properly, equally subtracting this change in mass from the remaining links to maintain the same overall robot mass. While this method introduces error into the model, experimental testing has shown acceptable performance.

B. Simulator Validation

To determine the accuracy of the simulation model and establish confidence in its use as a design tool, the simulation model was compared to the CAD and measured mass of the robot. The ESCHER hardware weighs 77.5 kg on a hanging crane scale, 74.7 kg in CAD, 77.5 kg in simulation. Force-torque sensors mounted in the ankles measure the majority of the robot mass during balancing at 76.4 kg not including the two 0.5 kg feet. The CAD model does not include any of the wiring for the robot, which is the primary source of variability in the mass measurements. The low variance between hardware, software, simulation, and sensor mass measurements establish a high level of confidence in the mass distribution of the simulator model.

A second validation experiment was conducted with THOR to compare the torque modeling of the simulator to measurements on hardware. The robot center of mass (COM) was commanded downward to squat at varying heights, using the whole-body controller developed by Hopkins et al. [15], and the required knee torques to maintain the height of each static pose were recorded. Fig. 2 contains the required knee torque across a range of hip joint heights from simulation and hardware testing. While this test only covers static cases, the simulated torque prediction tracked closely with the hardware data, furthering confidence in the accuracy of the simulator model for dynamic scenarios.

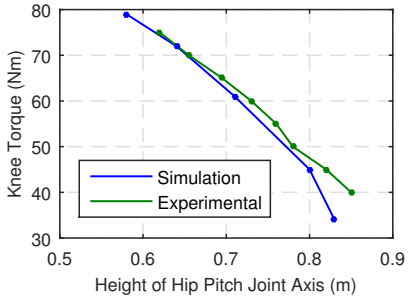

Fig. 2. Comparison of knee torque required to maintain squatting pose of various heights between simulation and hardware testing.

C. Design Requirements from Simulation

Hardware testing of THOR consistently overloaded the knee joint while stepping up onto objects similar to that shown in Fig. 3. Simulation of THOR in Gazebo revealed that stair stepping approached peak torque limits in the hip pitch and surpassed them in the knee, as shown in Fig. 4. Anticipating upper body modifications, a thigh redesign was proposed to support the additional weight across rough terrain. The validated Gazebo simulator derived hip and knee pitch torque and power requirements for the ESCHER thigh redesign. These were predicted using a weight-modified THOR for the worst-case walking terrain expected at the DRC final, which was the terrain in Fig. 3 that included a 23 cm step. The final mass of ESCHER was unknown at this stage of preliminary design, so each iteration added mass to the chest to increase the overall robot mass in 5 kg increments between 60 and 85 kg.

Joint positions, velocities, and torques were recorded for each robot mass and were used to determine critical joint angles requiring maximum torque. Fig. 4 contains joint

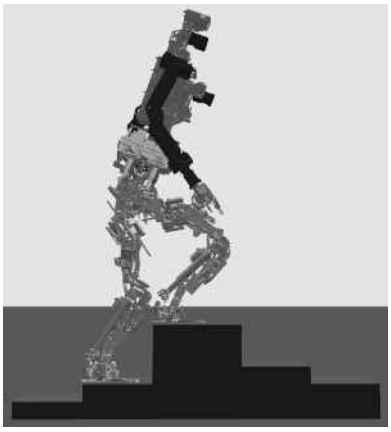

Fig. 3. Simulated weight-modified THOR stepping across varied terrain.

torque data collected through simulated walking over the terrain from Fig. 3 using the 60 kg THOR and the 85 kg robot model, the maximum expected mass of ESCHER. From this data, the new hip pitch joint should support a peak torque of 130 Nm at –85 deg, while the knee joint should support a peak torque of 195 Nm at 110 deg. Potential actuator configurations were evaluated using this design envelope to determine the overall factor of safety during stepping.

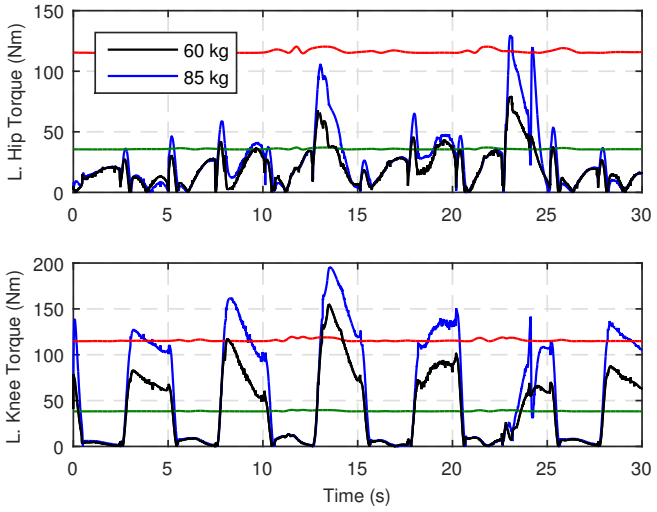

Fig. 4. Joint torque data from stepping simulations. Required joint torques are shown for the 60 and 85 kg robot models. Continuous (green) and peak (red) joint torque limits from THOR are overlaid based on joint angle.

III. ESCHER Upgrades

ESCHER is a platform built upon numerous upgrades from the THOR design. Table I highlights differences between ESCHER and THOR. ESCHER continues to use linear SEAs in each 6-DOF leg, and features new impedance-controlled 7-DOF arms and 4-DOF hands, a new chest design with four quad-core computers and batteries, and a new thigh with the torque to support the heavier platform.

TABLE I
Comparison of THOR and ESCHER

	THOR	ESCHER
Mass (kg)	61.3	77.5
Height (m)	1.78	1.78
Arm Span (m)	2.06	2.41
Processors	2x i7–4700E	2x i7–4700E
	1x i7–4770R	2x i7–4770R
Battery Capacity (Wh)	N/A	710
Arm DOF	9	11
Total DOF	34	38

A. Upper Body

The DRC finals featured tasks which increased focus on manipulation speed and autonomy. The arms used on THOR consisted of ROBOTIS Dynamixel Pro motors arranged in a 7-DOF configuration and outfitted with custom 2-DOF underactuated grippers [16]. With a 2 m wingspan and weighing 6.6 kg each, the Dynamixel Pro arms had limited payload capacity and lack joint torque sensing. Reachability analysis led to the decision to pursue 8.3 kg Adroit manipulator arms made by HDT Global, which have a more kinematically advantageous yaw-pitch-roll wrist configuration, an increased 2.4 m arm span, reliable through-actuator wiring, and support for joint impedance control. Fig. 5 shows results of a reachability study conducted using OpenRAVE [17] to compare the two arm configurations, highlighting the advantages of the longer arm links and new wrist configuration.

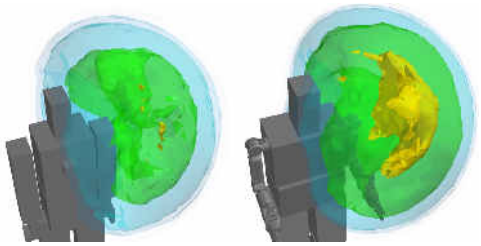

Fig. 5. Reachability regions of right hand of THOR (left) and ESCHER (right). Warmer colors represent a higher number of kinematic solutions to each desired target pose. Reprinted from [18] with permission.

The Adroit manipulators were developed from the DARPA Revolutionizing Prosthetics Program to advance the design and control of prosthetic limbs, and they have been used in a variety of commercial applications including bomb disposal. Each 7-DOF Adroit arm includes a 4-DOF manipulator featuring an opposable thumb and force sensing to determine grip. These extra degrees of freedom allowed for more potential grasp approaches and novel impedance control techniques for tasks such as door opening.

The increased perception and autonomy capabilities required for the DRC finals increased the necessary computational power carried onboard. The design of ESCHER took into account the processing capabilities of competitor systems, as well as overhead to enable expansion of capabilities for future research. The ESCHER chest was

upgraded to house two desktop-class Gigabyte BRIX PCs and two laptop-grade ADL-QM87PCs, each with quad-core i7 processors. With this change, power consumption of the onboard computing became the largest driver of battery capacity. The chest contains four 8 Ah 22.2 V Lithium Polymer batteries to allow a 1.5 hour runtime with a factor of safety of two based on worst case power analysis.

B. Lower Body

The THOR thigh design featured linear SEAs serially driving the hip pitch and knee joints through Hoeken's linkages: a novel four-bar mechanism optimized to provide a constant torque profile through up to 150 degrees of joint rotation [19]. The Hoeken's linkage generates a mechanical advantage directly proportional to the mechanism size; however, the linkages on THOR could not be scaled large enough within the thigh to generate sufficient torque to support the upper body modifications for the DRC finals. The solution for ESCHER was to redesign the thigh assembly which housed these two degrees of freedom, deriving design requirements from the simulation model as described in Section II.

With functional SEAs designed, manufactured, and tested for THOR it was desired to adapt the existing SEAs for use in the ESCHER thigh to reduce development time, cost, and project risk. Modified versions of the ankle actuators were used in the thighs and are serially connected to each joint through a simple 75 mm or 0.075m lever arm to selectively position the peak mechanical advantage at critical joint angles identified in Section II; this method mimics the torque profile of the human knee [20]. Fig. 6 includes plots of the peak and continuous torque profiles of the THOR and ESCHER hip pitch and knee joints. One downside to the elimination of the Hoeken's linkages was a small loss in joint range of motion. Table II contains a comparison of the range of motion between the THOR and ESCHER thighs. The pelvis and ankles remained the same between THOR and ESCHER.

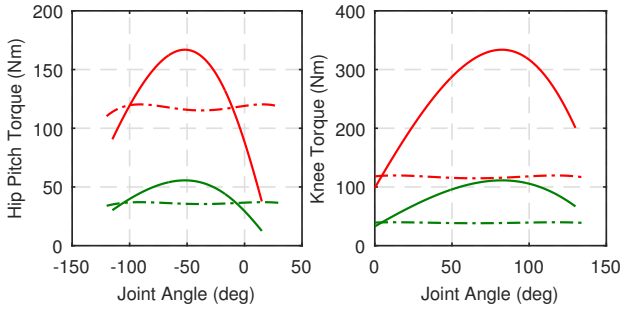

Fig. 6. Graphs showing continuous (green) and peak (red) torque limits over the range of motion available on the THOR (dashed) and ESCHER (solid) hip and knee pitch joints.

Simple torque curve tuning did not produce sufficient peak torque to meet design requirements in the knee given the peak actuator force of 2250 N. One option was to incorporate a motor with a higher peak torque or to decrease the actuator ball screw lead to produce a larger gearing ratio, but this would have negative effects on the velocity and backdrivability of the joint. Instead, double actuation was used at the knee joint, arranging two identical linear SEAs in a parallel configuration to power the single degree of freedom. This design doubles available joint torque using SEAs similar to those on THOR to reduce design complexity, development time, and cost. Fig. 7 contains renderings of the final thigh design that housing the hip pitch and knee actuators.

TABLE II
THIGH RANGE OF MOTION COMPARISON.

Joint	THOR	ESCHER
Hip Pitch (deg)	–120	–115
	30	15
Knee Pitch (deg)	0	0
	135	130

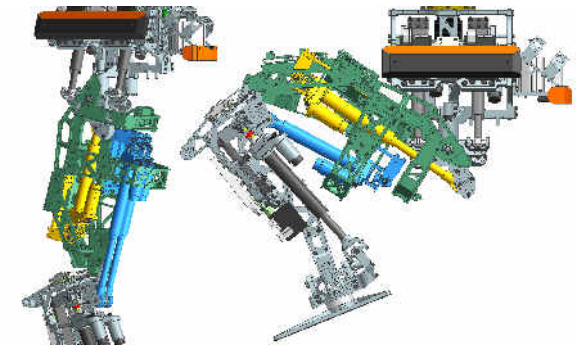

Fig. 7. CAD rendering of the ESCHER with covers removed, highlighting the thigh (green), hip pitch (yellow), and double knee actuators (blue).

Grimmer et al. [21] showed that using double actuation can reduce the individual force and peak power requirements of each actuator in a given joint. Park et al. [22] designed HUBO using two motors in the knee joint to meet high speed and torque requirements, noting the benefits of joint torque amplification with sustained speed. Additionally, Hitt et al. [23] used two linear SEAs for a 1-DOF ankle prosthesis, but required the development of additional control systems to synchronize both motors. Similar to the approach used in the parallel hip roll/yaw and ankle pitch/roll joints, control is implemented through equal distribution of forces across each actuator driven by the two-axis motor controller developed by Ressler [24]and requires no additional modifications to the embedded joint-space control approach described in [25]. Relying on independent force controllers for each actuator, this approach easily compensates for variable levels of friction present in each transmission, and eliminates the necessity for motor synchronization via a master/slave mode.

IV. RESULTS

Validation of the SEA force controller in a double actuation configuration was conducted on a representative knee joint attached to a rigid test stand, displayed in Fig. 8. With

the joint locked out to prevent rotation, a force tracking test was conducted to investigate the force difference between the two actuators using the controller developed for THOR [25]. Fig. 9 contains force response data to a 500 N chirp sweep from 0.1 Hz to 10 Hz over 10 seconds. While tracking error grows in the higher frequencies, the individual actuator force difference remains low, at worst case 40 N during transience.

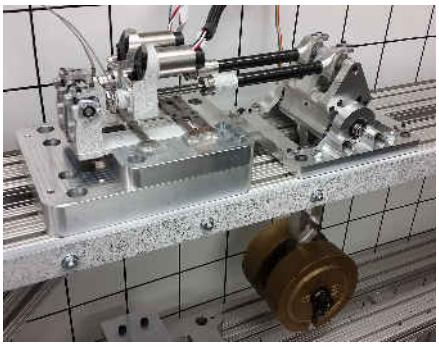

Fig. 8. Double actuator test stand arrangement.

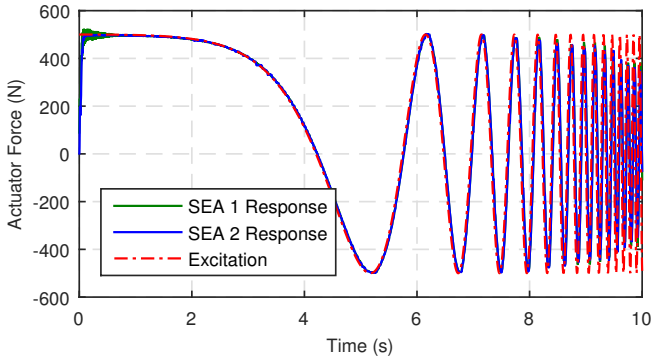

Fig. 9. Double actuator responses to 500 N chirp sweep excitation from 0.1 Hz to 10 Hz.

ESCHER stepped onto a 23 cm step in both simulation and in hardware as a validation of both the thigh redesign and simulation model. Fig. 10 includes critical segments of the stepping experiment. Fig. 11 contains graphs of the measured torque values overlayed with peak and continuous torque limits for the hip and knee pitch joints during the stepping cycle. Improvements to the whole-body controller to incorporate toe-off for vertical stepping, described in [26] have reduced individual joint torque demand by over 25% from the original simulation experiments performed in Section II. While both joints exhibit torques briefly overloading the continuous limit of the actuator motors, peak torque demand tends to occur at joint angles which have the highest available mechanical advantage and factor of safety.

Fig. 12 includes a plot of hip pitch and knee joint torques required while stepping onto the 23 cm block, comparing predictions from simulation to measured torques on hardware.

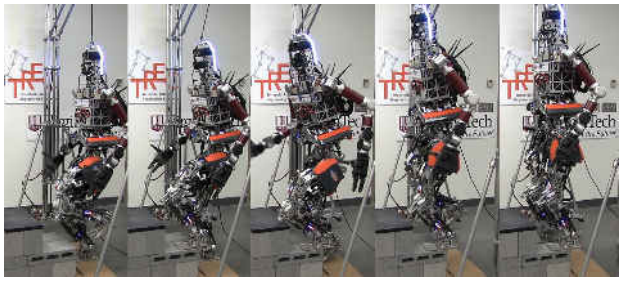

Fig. 10. Motion sequence of ESCHER stepping onto 23 cm step.

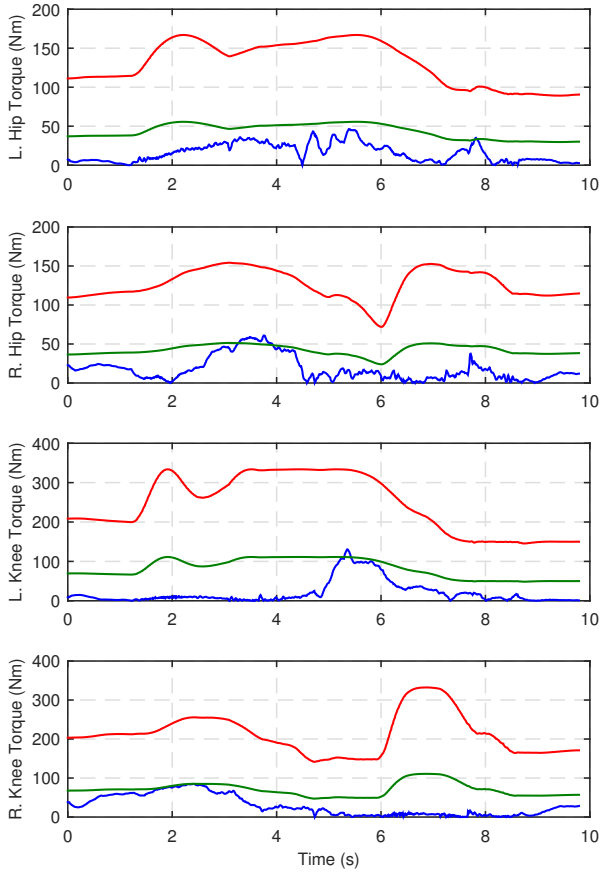

Fig. 11. Measured joint torques (blue) for hip and knee pitch joints during stepping onto 23 cm block. Continuous (green) and peak (red) joint torque limits from ESCHER are overlaid based on joint angle.

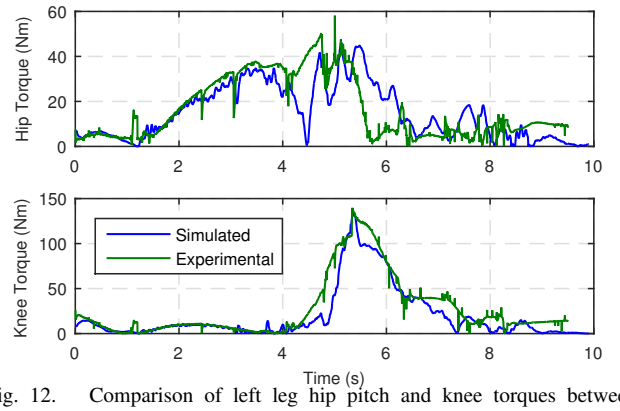

Fig. 12. Comparison of left leg hip pitch and knee torques between hardware and simulation when stepping onto 23 cm step.

V. Conclusions

The methodology presented in this paper produced an advanced electromechanical humanoid capable of completing the tasks of the DARPA Robotics Challenge. Traditional design methodologies using iterative practices would have been too time consuming on the compressed ESCHER design time line. By utilizing simulation for predicted performance, and due to the capability of SEAs to operate in parallel, ESCHER went from initial design to completed humanoid in only 10 months.

Approximations made in the humanoid simulation model, such as distributing variance in measured robot mass across body links, had little effect on performance, predicting static joint torques to within 10 Nm of hardware experiments. Simulated walking tests across challenging terrain determined peak joint torque and range of motion requirements. This informed mechanical design and allowed for the efficient placement of linear actuators, guaranteeing maximum torque at critical joint angles.

The robustness of SEA force control allowed for rapid scaling of power output at the knee joint. The high-frequency noise rejection and high force bandwidth of the SEAs and custom two-axis motor controller allowed implementation of a double actuation arrangement, effectively doubling knee torque without necessitating development of new control schemes.

Acknowledgments

This work is supported by ONR through grant N00014-11-1-0074 and by DARPA through grant N65236-12- 1-1002.

References

[1] A. Zoss, H. Kazerooni, and A. Chu, "Biomechanical design of the berkeley lower extremity exoskeleton (BLEEX)," *IEEE/ASME Transactions on Mechatronics*, vol. 11, no. 2, pp. 128–138, 2006.

[2] J. Perry, J. Rosen, and S. Burns, "Upper limb powered exoskeleton design," *IEEE/ASME Transactions on Mechatronics*, vol. 12, no. 4, pp. 408–417, 2007.

[3] A. Takanishi, Y. Ogura, and K. Itoh, "Some issues in humanoid robot design," in *International Symposium of Robotics Research*, San Francisco, CA, October 12-15 2005, pp. 357–372.

[4] T. Bushmann, S. Lohmeier, and H. Ulbrich, "Humanoid robot Lola: Design and walking control," *Journal of Physiology-Paris*, vol. 103, no. 3-5, pp. 141–148, 2009.

[5] K. Kaneko, F. Kanehiro, M. Morisawa, K. Akachi, G. Miyamori, A. Hayashi, and N. Kanehira, "Humanoid robot HRP-4 - humanoid robotics platform with lightweight and slim body," in *IEEE/RSJ International Conference on Intelligent Robots and Systems (IROS)*, San Francisco, CA, September 25-30 2011, pp. 4400–4407.

[6] J. Englsberger, A. Werner, C. Ott, B. Henze, M. Roa, G. Garofalo, R. Burger, A. Beyer, O. Eiberger, K. Schmid, and A. Albu-Schaffer, "Overview of the torque-controlled humanoid robot TORO," in *IEEE-RAS International Conference on Humanoid Robots (Humanoids)*, Madrid, Spain, November 18-20 2014, pp. 916–923.

[7] D. Gouailler, V. Hugel, P. Blazevic, C. Kliner, J. Monceaux, P. Lafoureade, B. Marnier, J. Serre, and B. Maisonnier, "Mechatronic design of NAO humanoid," in *IEEE/RSJ International Conference on Intelligent Robots and Systems (IROS)*, Kobe, Japan, May 12-17 2009, pp. 769–774.

[8] N. Koenig and A. Howard, "Design and use paradigms for Gazebo, an open-source multi-robot simulator," in *Intelligent Robots and Systems (IROS 2004), IEEE/RSJ International Conference on*, vol. 3, Sept 2004, pp. 2149–2154.

[9] A. Dietrich, T. Wimbock, and A. Albu-Schaffer, "Dynamic whole-body mobile manipulation with a torque controlled humanoid robot via impedance control laws," in *IEEE/RSJ International Conference on Intelligent Robots and Systems (IROS)*, San Francisco, CA, September 25-30 2011, pp. 3199–3206.

[10] J. Kim, H. Kwak, H. Lee, K. Seo, B. Lim, M. Lee, J. Lee, and K. Roh, "Balancing control of a biped robot," in *IEEE International Conference on Systems, Man and Cybernetics (SMC)*, Seoul, Korea, October 14-17 2012, pp. 2756–2761.

[11] L. Sentis, J. Petersen, and R. Philippsen, "Implementation and stability analysis of polarized whole-body compliant controllers on a wheeled humanoid robot in uneven terrains," *Autonomous Robots*, vol. 35, no. 4, pp. 301–319, 2013.

[12] M. Hutter, C. Gehring, M. Hopflinger, M. Blosch, and R. Siegwart, "Toward combining speed, efficiency, versatility, and robustness in an autonomous quadruped," *IEEE Transactions on Robotics*, vol. 30, no. 6, pp. 1427–1440, 2014.

[13] N. Paine, J. Mehling, J. Holley, N. Radford, J. Gwendolyn, C. Fok, and L. Sentis, "Actuator control for the nasa-jsc valkyrie humanoid robot: A decoupled dynamics approach for torque control of series elastic robots," *Journal of Field Robotics*, vol. 32, no. 3, pp. 378–396, 2015.

[14] V. Orekhov, C. Knabe, M. Hopkins, and D. Hong, "(Forthcoming). An unlumped model for linear series elastic actuators with ball screw drives," in *IEEE/RSJ International Conference on Intelligent Robots and Systems (IROS)*, Hamburg, Germany, Sep 28-Oct 03 2015.

[15] M. Hopkins, D. Hong, and A. Leonessa, "Compliant locomotion using whole-body control and divergent component of motion tracking," in *IEEE International Conference on Robotics and Automation (ICRA)*, Seattle, Washington, May 26-30 2015.

[16] M. Rouleau and D. Hong, "Design of an underactuated robotic end-effector with a focus on power tool manipulation," in *ASME International Design Engineering Technical Conferences (IDETC)*, Buffalo, NY, August 17-20 2014, pp. 1–7.

[17] R. Diankov and J. Kuffner, "OpenRAVE: A planning architecture for autonomous robotics," Robotics Institute, Carnegie Mellon University, Tech. Rep. CMU-RI-TR-08-34, 2008.

[18] N. Wittenstein, "Force feedback for reliable robotic door opening," Master's thesis, Virginia Polytechnic Institute and State University, Blacksburg, Virginia, 2015.

[19] C. Knabe, B. Lee, and D. Hong, "An inverted straight line mechanism for augmenting joint range of motion in a humanoid robot," in *ASME International Design Engineering Technical Conferences (IDETC)*, Buffalo, New York, August 17-20 2014, pp. 1–6.

[20] G. Caldwell, W. Adams, and M. Whetstone, "Torque/velocity properties of human knee muscles: Peak and angle-specific estimates," *Canadian Journal of Applied Physiology*, vol. 18, no. 3, pp. 274–290, 1993.

[21] M. Grimmer, M. Eslamy, S. Gliech, and A. Seyfarth, "A comparison of parallel- and series elastic elements in an actuator for mimicking human ankle joint in walking and running," in *IEEE International Conference on Robotics and Automation (ICRA)*, Saint Paul, Minnesota, May 14-18 2012, pp. 2463–2470.

[22] I. Park, J. Kim, J. Lee, and J. Oh, "Mechanical design of the humanoid robot platform HUBO," *Journal of Advanced Robotics*, vol. 21, no. 11, pp. 1305–1322, 2007.

[23] J. Hitt, J. Merlo, J. Johnston, M. Holgate, A. Boehler, K. Hollander, and T. Sugar, "Bionic running for unilateral transtibial military amputees," in *27th Army Science Conference (ASC)*, Orlando, Florida, November 29 - December 2 2010, pp. 1–8.

[24] S. Ressler, "Design and implementation of a dual axis motor controller for parallel and serial series elastic actuators," Master's thesis, Virginia Polytechnic Institute and State University, Blacksburg, Virginia, Mar. 2014.

[25] M. Hopkins, C. Knabe, S. Ressler, and D. Hong, "(Forthcoming). Embedded joint-space control of a series elastic humanoid," in *IEEE/RSJ International Conference on Intelligent Robots and Systems (IROS)*, Hamburg, Germany, Sep 28-Oct 03 2015.

[26] M. Hopkins, R. Griffin, A. Leonessa, B. Lattimer, and T. Furukawa, "(Forthcoming). Design of a compliant bipedal walking controller for the DARPA Robotics Challenge," in *Humanoid Robots (Humanoids), 15th IEEE-RAS International Conference on*, 2015.